

Myelin Breakdown and Iron Changes in Huntington's Disease: Pathogenesis and Treatment Implications

George Bartzokis · Po H. Lu · Todd A. Tishler ·
Sophia M. Fong · Bolanle Oluwadara · J. Paul Finn ·
Danny Huang · Yvette Bordelon · Jim Mintz ·
Susan Perlman

Accepted: 5 April 2007
© Springer Science+Business Media, LLC 2007

Abstract

Background Postmortem and in vivo imaging data support the hypothesis that premature myelin breakdown and subsequent homeostatic remyelination attempts with increased oligodendrocyte and iron levels may contribute to Huntington's Disease (HD) pathogenesis and the symmetrical progress of neuronal loss from earlier-myelinating striatum to later-myelinating regions. A unique combination of in vivo tissue integrity and iron level assessments was used to examine the hypothesis.

Methods A method that uses two Magnetic resonance imaging (MRI) instruments operating at different field-strengths was used to quantify the iron content of ferritin molecules (ferritin iron) as well as tissue integrity in eight regions in 11 HD and a matched group of 27 healthy control subjects. Three white matter regions were selected based on their myelination pattern (early to later-myelinating) and fiber composition. These were frontal lobe white matter

(Fwm) and splenium and genu of the corpus callosum (Swm and Gwm). In addition, gray matter structures were also chosen based on their myelination pattern and fiber composition. Three striatum structures were assessed [caudate, putamen, and globus pallidus (C, P, and G)] as well as two comparison gray matter regions that myelinate later in development and are relatively spared in HD [Hippocampus (Hipp) and Thalamus (Th)].

Results Compared to healthy controls, HD ferritin iron levels were significantly increased in striatum C, P, and G, decreased in Fwm and Gwm, and were unchanged in Hipp, Th, and Swm. Loss of tissue integrity was observed in C, P, Fwm, and especially Swm but not Hipp, Th, G, or Gwm. This pattern of findings was largely preserved when a small subset of HD subjects early in the disease process was examined.

Conclusions The data suggest early in the HD process, myelin breakdown and changes in ferritin iron distribution

G. Bartzokis · P. H. Lu · T. A. Tishler · S. M. Fong ·
B. Oluwadara · Y. Bordelon · S. Perlman
Department of Neurology, The David Geffen School
of Medicine at UCLA, Los Angeles, CA 90095, USA

G. Bartzokis
Laboratory of Neuroimaging, Department of Neurology,
Division of Brain Mapping, UCLA, Los Angeles, CA 90095,
USA

G. Bartzokis · P. H. Lu · T. A. Tishler · S. M. Fong ·
B. Oluwadara
Department of Psychiatry, Greater Los Angeles VA Healthcare
System, West Los Angeles, CA 90073, USA

T. A. Tishler
Neuroscience Interdepartmental Graduate Program, The David
Geffen School of Medicine at UCLA, Los Angeles, CA 90095,
USA

J. P. Finn
Department of Radiology, The David Geffen School of Medicine
at UCLA, Los Angeles, CA 90095, USA

D. Huang
Department of Neurology and Biobehavioral Sciences,
The David Geffen School of Medicine at UCLA, Los Angeles,
CA 90095, USA

J. Mintz
Department of Psychiatry and Biobehavioral Sciences,
The David Geffen School of Medicine at UCLA, Los Angeles,
CA 90095, USA

G. Bartzokis (✉)
UCLA Alzheimer's Disease Center, 10911 Weyburn Avenue
Suite 200, Los Angeles, CA 90095-7226, USA
e-mail: gbar@ucla.edu

underlie the pattern of regional toxicity observed in HD. Prospective studies are needed to verify myelin breakdown and increased iron levels are causal factors in HD pathogenesis. Tracking the effects of novel interventions that reduce myelin breakdown and iron accumulation in pre-clinical stages of HD could hasten the development of preventive treatments.

Keywords Brain · Neurodegeneration · Ferritin · FDRI · Huntingtin · BDNF · Excitotoxicity · Prevention · Onset · Oligodendrocyte

Abbreviations

AD	Alzheimer's disease
C	Caudate
CNS	Central nervous system
BDNF	Brain-derived neurotrophic factor
FDRI	Field-dependent R_2 increase (an in vivo MRI measure of ferritin iron)
Fwm	Frontal lobe white matter
G	Globus pallidus
Gwm	Genu of the corpus callosum white matter
HD	Huntington's disease
Hipp	Hippocampus
MRI	Magnetic resonance imaging
P	Putamen
R_2	Transverse relaxation rate (an in vivo MRI measure of myelin breakdown)
Swm	Splenium of the corpus callosum white matter
Th	Thalamus

Introduction

Huntington's disease (HD) is a genetic neuropsychiatric disorder that causes behavioral, cognitive, and motor dysfunction. The disease is caused by the abnormal repetition of a CAG trinucleotide sequence encoding for a polyglutamine tract at the N-terminal of the gene coding for a protein named huntingtin [for review see 1–3].

Huntington's disease is autosomal dominant and the presence of a single allele with more than 37 CAG repeats causes disease but a double dose of the gene in homozygotes does not increase its rate of progression [4]. This suggests that mutant huntingtin contributes to reaching a threshold of toxicity and once the threshold is reached the progression is dependent primarily on mutation-independent factors [5, 6]. Supporting this contention are observations that the defective gene and its protein product are expressed throughout development, yet the typical HD phenotype is characterized by a peak risk of onset in

middle-age, suggesting a development-dependent process is involved in its pathogenesis [reviewed in 7].

The mutant huntingtin protein is ubiquitously present in most brain areas as well as the periphery, and is *not* noticeably present at higher levels in the neurons that degenerate first [8]. This implies that its primary impact may not be on neurons. The specific degeneration of myelinated projection neurons with sparing of interneurons suggests that a defect of myelination may be involved in its pathogenesis [7]. This hypothesis is supported by the literature documenting the presence of myelin breakdown in this disease, both in studies using in vivo imaging of subjects with HD [6, 9–15; reviewed in 7] and subjects with preclinical HD [16, 17], as well as *postmortem* methods [18–21] (see figure below for example of myelin breakdown in HD) (Fig. 1).

Furthermore, in HD neuronal degeneration begins in the caudate and putamen (C and P) striatum structures and then spreads in a predictable, bilateral, and symmetric pattern to involve other earlier-myelinating regions, leaving later-myelinating regions like the medial temporal lobe much less affected [for review see 1–3, 7].

These observations led to the hypothesis that the pathogenesis of the disease begins with a deleterious effect of the mutant huntingtin on myelination that results in the brain-specific, age-related, and symmetric spread of the disease [7]. This hypothesis will be summarized here. Once reciprocal myelinated neuronal circuits become functional, myelin breakdown results in failure of afferent

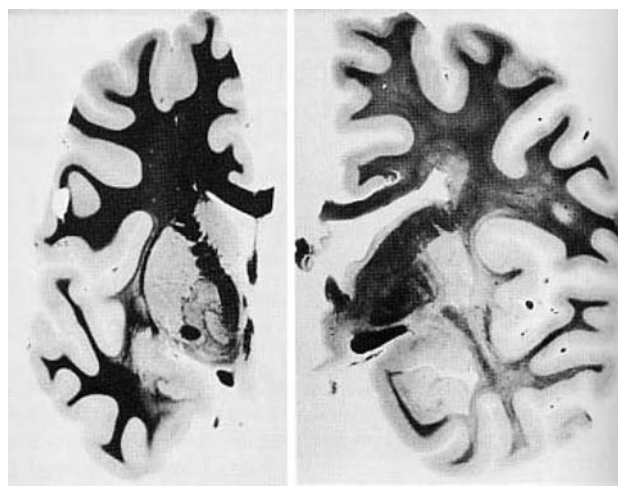


Fig. 1 Myelin Breakdown in Huntington's Disease Brain. *Postmortem* myelin stain (myelin is black). On the left side a coronal plane section through the frontal and temporal lobes of a normal brain. On the right side a section at the same level taken from a patient with Huntington's chorea that is magnified 2 \times . Note striking myelin breakdown and white matter atrophy in the HD brain (right) [from 18]

transmission causing the underlying neuron to be overstimulated by its efferent feedback. This excitotoxic process eventually destroys neurons with myelin defects. In HD, earlier myelinated axons, especially the ones of the striatum, bear the brunt of damage from mutant huntingtin [reviewed in 7]. (See discussion section for possible molecular mechanism.) Oligodendrocytes continue developing and increase their numbers throughout the human lifespan [22]. In HD, this physiologic attempt of oligodendrocytes to repair and remyelinate results in strikingly elevated numbers of oligodendrocytes years before the appearance of symptoms [23–25]. Iron is required for myelination and oligodendrocytes have the highest iron content of all brain cells [reviewed in 26, 27]. Thus, along with the increased oligodendrocyte numbers, in the HD brain there is an associated increase in iron levels in early myelinating regions like the basal ganglia [6, 20, 28, 29]. As suggested by Youdim and others [7, 30–34] the increased iron levels likely add to the neuronal excitotoxicity by promoting free radical toxicity.

This novel hypothesis of HD pathogenesis was tested *in vivo*. The breakdown in the structural integrity of myelin sheaths can be indirectly measured *in vivo* with transverse relaxation rate (R_2) Magnetic resonance imaging (MRI) measures. R_2 measures are markedly sensitive to small changes in the amount of tissue water [35, 36], which decreases R_2 , and tissue iron, which increases R_2 [37–40]. The lower R_2 caused by increases in tissue water is observed at any MRI field strength (magnet strength) and its magnitude is field-independent. Ultrastructural electron microscopy studies demonstrate that age-related myelin breakdown results in microvacuolations consisting of splits of myelin sheath layers that create microscopic fluid-filled spaces that increase MRI “visible” water and thus decrease R_2 [41–43].

On the other hand, the increases in R_2 caused by increases in tissue iron are field-dependent, being more pronounced as the field-strength of the MRI instrument increases [37–40, 44–47]. This field-dependent effect is unique and specific to ferritin molecules in which the bulk of brain iron is stored [48, 49]. This property of ferritin was used in an *in vivo* MRI method called field-dependent R_2 increase (FDRI) that can obtain highly specific and reproducible measures of the iron content of ferritin molecules (ferritin iron) [37, 38]. Briefly, the FDRI measure is calculated as the difference in R_2 values obtained with two different field-strength MRI instruments, divided by the difference in the two field strengths. The FDRI measure is represented graphically by the slope of the line when R_2 is plotted versus field strength. When the difference in field strengths is 1 T (as is the case when a 0.5 and a 1.5 T instrument are used) the FDRI is simply the difference in

R_2 between the two instruments [37, 38]. FDRI has been shown to be independent of the amount of iron loading (number of iron atoms per molecule of ferritin) [47], to increase linearly with field-strength [37, 40, 46, 47], and be very highly correlated ($r > 0.97$) with *postmortem* measures of brain tissue iron [38, 50, 51]. Thus, FDRI is a specific measure of the total iron contained in ferric oxyhydroxide particles that form the mineral core of ferritin molecules. In human tissue, ferritin and its breakdown product (hemosiderin) are the only known physiologic sources of such particles [37, 39, 46, 52]. The FDRI measure will therefore be referred to herein as ferritin iron [6, 50, 53].

Emerging treatments for degenerative brain diseases (such as iron chelation and antioxidants) make *in vivo* regional assessments of iron levels and myelin integrity essential for rational planning of such interventions [27, 54, 55]. We therefore tested the above myelin hypothesis on the pathogenesis of HD by assessing additional regions of interest from an existing dataset [6]. The splenium and genu of the corpus callosum (Swm and Gwm) were assessed as regions that have primarily larger heavily myelinated and smaller lightly myelinated fibers, respectively [56, 57], as well as the frontal lobe white matter (Fwm) that contains a mixture of both types of fibers. The early myelinating neostriatal structures C, P and globus pallidus (G), as well as two later-myelinating comparison gray matter regions that are relatively spared in HD [Hippocampus (Hipp) and Thalamus (Th)] [1, 58], were also assessed.

Experimental procedure

The subject samples have been described in detail elsewhere [6] and will only be summarized here. All subjects participated after being fully informed of the study and giving written consent.

Subjects with HD

Prior to referral into the study, the subjects with HD underwent complete clinical assessment, and the diagnosis was confirmed by an experienced neurologist (S.P.) via a thorough review of their history and clinical evaluation. The HD subjects had a family history and/or genetic test positive for HD. Eleven Caucasian subjects (seven men and four women) ranging in age from 25 to 67 years (mean age \pm SD, 46.2 \pm 11.9 years) and symptomatic from 0.75 to 20 years (mean \pm SD, 7.8 \pm 6.3 years) completed the study. The sample size was not computed *a priori*.

Healthy control subjects

To control for the effects of age on the dependent measures we selected cases from a pool of normal control subject volunteers recruited from the community and hospital staff [51]. Normal subjects were excluded if there was a family history of a degenerative brain disorder, or a history of head trauma resulting in loss of consciousness for longer than 15 min. Normal subjects were included if they fell in the demographic parameters (age range and race) of the HD group and none was excluded on the basis of MRI findings. This comparison group initially consisted of 27 subjects, but one subject was later discovered to have had a history of traumatic brain injury with loss of consciousness of longer than 15 min; he was thus excluded from the present analysis. The final control sample consisted of 26 subjects (22 men and four women) ranging in age from 26 to 69 years (mean age \pm SD, 45.2 ± 16.5 years). The subjects with HD and control subjects did not differ in mean age either in the overall or in sex-specific groups ($P > 0.5$).

MRI protocol

The methods have been described in detail elsewhere [6, 38] and will be briefly summarized here. All subjects were scanned using the same two MRI instruments (1.5 and 0.5 T), and the two scans were done within 1 h of each other using the same imaging protocol. Two pilot sequences were obtained to specify the location and spatial orientation of the head and the position of the axial image acquisition grid. A mid-sagittal image was used to position the axial image acquisition grid. The axial image acquisition sequence acquired interleaved contiguous slices using a Carr Purcell Meiboom Gill dual spin-echo sequence of 2500/20,90/2 (RT/TE/excitations), 3 mm slice thickness, 192 gradient steps, and 25 cm field of view. The pilot scans obtained prior to the axial image acquisition were used to determine the alignment and accuracy of head repositioning in the second MRI instrument. To consistently position the actual image slices identically within the brain and thus sample the same volume of tissue, the axial slice-select grid was adjusted so that the anterior commissure was contained within the same slice in both high-field (1.5 T) and low-field (0.5 T) instruments. For increased consistency all subsequent measures were referenced to this slice [38].

Image analysis

The image analysis software operating on a Macintosh-configured image analysis workstation permitted the rater, who was blind to diagnosis and demographic data, to

delineate the region of interest (ROI) using a mouse. The contour of the ROI cross-sectional area was drawn using the gray/white matter contrast of the early echo (TE = 20) images. The ROI was then transferred to gray-scale encoded transverse relaxation time (T_2) maps in which each brain voxel was produced by an automated algorithm using the two signal intensities (echo times, 20 and 90 ms) of the dual spin-echo sequence [38]. The R_2 was calculated as the reciprocal of $T_2 \times 1,000$. The average R_2 of the two slices from both hemispheres was the final measure used in the subsequent analyses. The FDRI measure was calculated as the difference in R_2 (high-field R_2 –low-field R_2). Test–retest reliability for FDRI measures was very high with intraclass correlation coefficients ranging from 0.88 to 0.99 ($P < 0.0023$) [38].

Statistical methods

The FDRI means in the normal and HD groups were compared using a factorial analysis of covariance design. Because of the known increases in brain iron levels and FDRI with advancing age [38, 59], and the possibility that sex may also affect age-related changes in FDRI [51], sex and age (a continuous variable) were included as covariates in the statistical designs. The inclusion of the covariates did not change the results substantively. Separate analyses were done in each of the eight ROIs. The low-field R_2 measure of tissue integrity in the two groups was also examined using the same multiple discriminant (regression) models, again controlling for sex and age. In order to ascertain whether these differences existed early in the disease process, the above analyses were rerun using only the sample of HD subjects whose illness length was < 2 years.

In follow-up analyses of white matter iron changes, Pearson correlations (partialling out age and gender) between diagnosis and FDRI were computed in each white matter region, yielding a standardized index of the size of the group difference. Pairwise comparisons of the correlation coefficients among the three white matter regions were performed using Hotelling's statistic [60], a test for the difference between two non-independent correlations [61].

Results

The HD group had significantly elevated mean FDRI in all three basal ganglia regions, but not in the other two gray matter regions (Th or Hipp) that are relatively spared in HD. The white matter regions showed the reverse pattern with significantly *decreased* FDRI in the Fwm and Gwm

and a non-significant increase in the Swm (Table 1 and Fig. 2a). The diagnostic group difference in FDRI of Swm (increase) was significantly different from the decreases in Fwm ($t_{34} = 2.28, P = 0.03$) and Gwm ($t_{34} = 2.60, P = 0.01$).

When the FDRI data on the subgroup with 2 years illness duration or less was assessed, a similar pattern was observed (with the exception of Fwm) with elevations in ferritin iron for C ($F = 30.7, P < 0.0001$), P ($F = 13.84, P = 0.001$), and G ($F = 24.5, P < 0.0001$), decline for Gwm ($F = 4.5, P = 0.044$), and no significant differences in the remaining regions (all regions $df = 1, 25$ except Hipp where $df = 1, 24$).

The low-field R_2 data were examined as a measure of changes in tissue integrity. In the overall sample (Table 2 and Fig. 2b) R_2 was significantly lower in the HD group in

the neostriatum (C and P) gray matter regions, and was also lower in the Swm and Fwm regions. When the data on the subgroup with 2 years illness duration or less was assessed, a similar pattern was observed (with the exception of Fwm) with declines in R_2 for C ($F = 6.0, P = 0.022$), P ($F = 8.6, P = 0.007$), and Swm ($F = 5.6, P = 0.03$), and no significant differences in the remaining regions (all regions $df = 1, 25$ except Hipp where $df = 1, 24$).

Discussion

The data show that the ferritin iron elevations that have also been observed in *postmortem* studies of HD [20, 28, 29] are specific to the earlier-myelinating striatum regions (C, P, and G) and are not present in the later-myelinating

Table 1 Ferritin iron levels (FDRI measure) in HD versus healthy control subjects

	HD patients (n = 11)		Normal controls (n = 26)		F	P
	Mean	SD	Mean	SD		
C	3.63	1.17	2.23	0.43	31.10	<0.0001
P	3.72	1.28	2.62	0.59	17.10	0.0001
G	5.97	1.30	4.46	0.63	22.40	<0.0001
Th	1.40	0.37	1.30	0.26	0.87	0.36
Hipp	0.62	0.20	0.70	0.21	1.70	0.20
Fwm	1.46	0.30	1.67	0.23	6.42	0.016
Gwm	0.86	0.30	1.28	0.36	11.10	0.002
Swm	1.14	0.48	1.08	0.32	0.15	0.70

Data are presented as the unadjusted mean and SD

F and P-values are based on analysis of covariance model with age and gender as covariates: $df = 1, 33$ for all regions except for Hipp ($n = 25$ for normal controls, $df = 1, 32$)

FDRI field dependent relaxation rate (R_2) increase

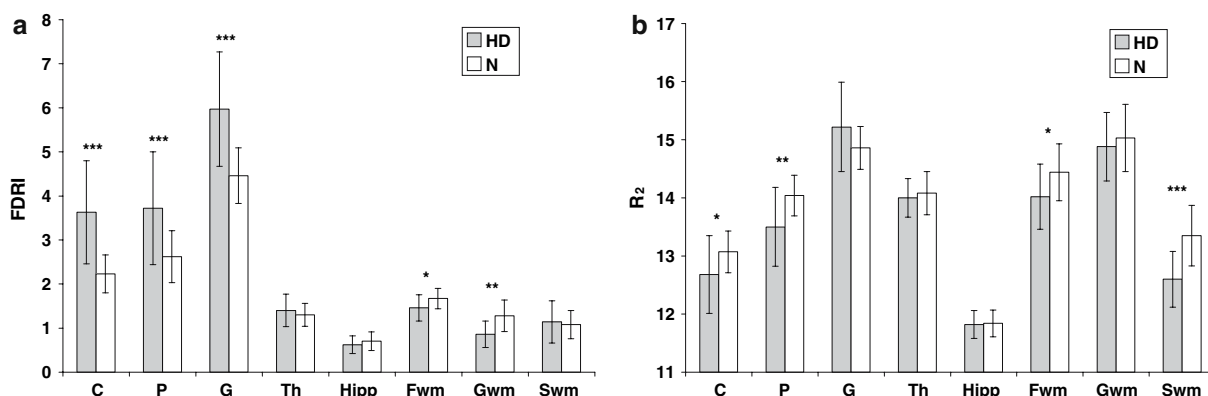


Fig. 2 a Ferritin iron levels (FDRI measure) in HD versus healthy control subjects. Data are presented as the unadjusted mean and SD. Statistical significance based on analysis of covariance model with age and gender as covariates: $df = 1, 33$ for all regions except for Hipp ($n = 25$ for normal controls, $df = 1, 32$). FDRI field dependent relaxation rate (R_2) increase. * $P < 0.05$; ** $P < 0.01$; *** $P < 0.001$.

b Tissue integrity (R_2 measures) in HD versus healthy control subjects. Data are presented as the unadjusted mean and SD. Statistical significance based on an analysis of covariance model with age and gender as covariates: $df = 1, 33$ for all regions except for Hipp ($n = 25$ for normal controls, $df = 1, 32$). R_2 Transverse relaxation rate. * $P < 0.05$; ** $P < 0.01$; *** $P < 0.001$

Table 2 Tissue integrity (R_2 measures) in HD versus healthy control subjects

	HD patients ($n = 11$)		Normal controls ($n = 26$)			
	Mean	SD	Mean	SD	F	P
C	12.68	0.67	13.07	0.36	7.00	0.012
P	13.50	0.68	14.04	0.35	10.90	0.002
G	15.22	0.77	14.86	0.37	3.37	0.08
Th	14.00	0.33	14.08	0.37	0.39	0.54
Hipp	11.82	0.24	11.84	0.23	0.06	0.81
Fwm	14.02	0.56	14.44	0.49	5.55	0.025
Gwm	14.88	0.59	15.03	0.58	0.60	0.440
Swm	12.60	0.48	13.35	0.52	16.10	0.0003

Data are presented as the unadjusted mean and SD

F and P -values are based on an analysis of covariance model with age and gender as covariates: $df = 1, 33$ for all regions except for Hipp ($n = 25$ for normal controls, $df = 1, 32$)

R_2 transverse relaxation rate

Th or Hipp regions (Table 1 and Fig. 2a). Regionally specific changes in ferritin iron are also observed in the three white matter regions (Table 1 and Fig. 2a). Compared to normal controls, the earlier-myelinating Swm region has non-significantly *higher* ferritin iron levels in HD in contrast to the significantly *lower* levels of later-myelinating regions (Fwm and Gwm).

The ferritin iron changes occurring in white matter regions, with significant differences between increased levels in the early myelinating Swm and declines in the later-myelinating Fwm and Gwm, are consistent with *postmortem* and *in vivo* imaging studies suggesting that in HD, brain degeneration may begin with myelin abnormalities [6, 9–21; reviewed in 7].

The possibility that dysregulated myelination is pathogenic to this disease is also supported by reports that presymptomatic HD brains show an *increase* (doubling) in the density of oligodendrocytes in the striatum years before striatal atrophy or loss of neurons occurs [24, 25]. This is consistent with our observations of regionally increased ferritin iron since oligodendrocytes have very high iron levels and their ability to differentiate and multiply is dependent on achieving high iron stores [reviewed in 7, 26]. Thus, earlier-myelinating regions such as C, P, G, and Swm show increased ferritin iron, consistent with attempts to remyelinate, and strikingly increased oligodendrocyte numbers that accumulate the necessary iron to support this process [24, 25]. Meanwhile, later-myelinating regions such as Hipp, Fwm, and Gwm tend to have numerically lower than expected ferritin iron levels. Even though not all these later-myelinating region ferritin iron declines reach statistical significance, this pattern suggests suboptimal iron availability possibly due to the diversion/redistribution of iron to the earlier-myelinating regions as homeostatic mechanisms are driving remyelination attempts (see

below). Studies with larger sample sizes are needed to clarify these observations.

The low-field R_2 data also support the possibility that myelin breakdown of early myelinating regions may represent a pathogenetic insult in HD. Low-field R_2 is much less sensitive to ferritin iron and declines in R_2 provide an excellent measure of the relative increase in tissue water that characterizes destructive brain processes [35, 36, 42]. As expected from the predilection of HD to destroy C and P, those striatal regions show significant R_2 reductions (loss of tissue integrity) that are absent in the other three gray matter regions (Table 2 and Fig. 2b). Thus, in these early myelinating gray matter regions loss of tissue integrity (which likely includes loss of myelin integrity) and increased iron co-occur (Fig. 2a, b). In the white matter regions the most striking declines are observed in the Swm and Fwm, with no significant declines observed in the Gwm. This pattern is consistent with myelin breakdown of early and heavily myelinated axons.

Unlike the Gwm where only small fibers are present, the Fwm and especially the Swm regions contain higher proportions of large, earlier- and heavier-myelinated axons [56]. The myelin breakdown we observed seems to disproportionately affect the two regions that contain such heavily myelinated fibers (a mixture of early and late-myelinating fibers in Fwm and almost exclusively early myelinating fibers in the Swm). As opposed to gray matter where a variety of cell bodies (neurons, astrocytes, and oligodendrocytes) and processes (axons, dendrites, and myelin) coexist, white matter regions are composed primarily of myelin and axons. Thus, the white matter data gives the clearest support for the hypothesized process of HD pathogenesis: breakdown of early and heavily myelinated myelin, homeostatic increase in oligodendrocytes attempting to remyelinate,

and the increase in iron levels caused by the increasing numbers of oligodendrocytes. The pattern of findings in early and later-myelinating gray matter regions is however almost identical to the pattern seen in the white matter suggesting that the same process is the most likely explanation (with some differences in magnitude) for the pattern observed in gray matter. It is noteworthy that in the subgroup of HD subjects whose illness duration was 2 years or less roughly this same pattern of significant gray and white matter ferritin iron differences as well as R_2 differences was observed as in the overall group. This suggests that differences in ferritin iron levels and myelin integrity are not merely an epiphenomenon of the disease process.

The molecular mechanisms through which mutant huntingtin could precipitate premature myelin breakdown that *preferentially* affects early and heavily myelinated axons and regions (Table 2) are worth considering [7]. The thick myelin sheaths of these axons depend on myelin basic protein for their integrity to a greater extent than smaller axons with thinner myelin sheaths [7, 62–64]. Expression of myelin basic protein is normally supported by brain-derived neurotrophic factor (BDNF) [65–67] that is distributed by vesicular axonal transport. Wild type huntingtin increases and mutant huntingtin interferes with axonal vesicular transport [68, 69] and thus could undermine myelin integrity by reducing trophic support. Intact oligodendrocyte differentiation [62] and homeostatic attempts to repair/remyelinate [22, 70] could cause both the excessive oligodendrocyte production [24, 25] and the associated iron accumulation [6, 20, 28, 29]. These repair mechanisms would mask myelin damage/loss and could also explain the underappreciation of myelin breakdown as an early event in the pathogenesis of HD and other brain diseases (Fig. 1) [reviewed in 7, 42, 71].

Alternative explanations for the increase in ferritin iron involving neurons, astrocytes, or microglia and oxidative stress are possible especially for the later disease stages. Oligodendrocytes are enriched in iron [72, 73] and have the highest ferritin content of all brain cell types [74–76]. By comparison neurons and astrocytes have relatively low ferritin levels [74, 76, 77]. The severity and progression of HD pathology is associated with increased microglia numbers and their activation [78, 79], however, although these cells can achieve high ferritin levels, their activation may decrease these levels [80, 81]. Our observation that increased ferritin iron is present very early in the HD disease process is consistent with the doubling of oligodendrocytes in presymptomatic HD [24, 25]. Together with the higher numbers of oligodendrocytes in healthy adult brain [22, 82], these factors make it likely that oligodendrocytes underlie the ferritin iron increases especially early in the disease process.

Important limitations of this study need to be considered. The cross-sectional design could underestimate some of the HD versus healthy control differences in FDRI and R_2 . This could happen if increased brain iron levels and loss of tissue integrity are associated with mortality and/or accelerated debilitation that caused patients to be excluded from, or unable to participate in or complete the study. In addition, in a cross-sectional study, only limited inferences can be made about any shifts in iron between regions or the causal relationship between changes in iron levels or tissue integrity and HD pathogenesis, and prospective studies in presymptomatic subjects are needed to verify causality. Finally, postmortem studies that integrate the examination of oligodendrocytes and other cellular components, their ferritin levels, and the integrity of myelin in early and late-myelinating structures are also needed to directly clarify the mechanisms of HD pathophysiology.

The search for viable therapies in HD as well as in other developmental diseases such as schizophrenia and degenerative diseases such as Alzheimer's disease (AD) has been hampered by the unique manifestation of these diseases in humans and limited research focus on the involvement of myelin [7, 26, 71, 83–85]. Myelin plays an essential role in vertebrate brain structure and function and the human brain is *uniquely* dependent on the elaboration of this late evolutionary invention. The unique vulnerabilities of myelin and the oligodendrocytes that produce it are directly pertinent to many uniquely human neuropsychiatric diseases, including many degenerative disorders such as HD and AD and the spreading of their pathognomonic lesions across the brain in patterns that, like myelination, are predictable, symmetric, bilateral, and specific to each disease [reviewed in 7, 26, 71; Bartzokis et al., unpublished data]. In this myelin-centered view of the human brain, the strikingly predictable *neuronal* degeneration pattern that is a pathognomonic feature of HD [86] is viewed as an epiphenomenon paralleling the spreading pattern of brain myelination and its premature breakdown, as described above [7].

In many degenerative brain diseases myelin breakdown and iron accumulation begin before the first appearance of pathological changes [reviewed in 26, 71]. There is therefore a decades-long period in which therapeutic interventions could modify the course of these diseases, before clinical evidence such as behavioral, cognitive, and motor decrements appear. Thus, it may be possible that medication development could be carried out in very early disease stages using non-invasive *in vivo* combined neuroimaging markers of both myelin breakdown and iron levels [26, 42, 71, 83]. Imaging biomarker methods could thus be used to target emerging therapeutic interventions such as chelators [87–91; for review see 27, 54, 55, 92–95] years before clinical disease manifestations [96]. This approach may be

especially effective in diseases such as HD and AD where genetic tests can identify individuals that will definitely develop the disease or subgroups that are at high risk. Early intervention may make it possible to increase effectiveness of treatments, decrease the need for later more aggressive approaches, and ultimately may represent a heretofore unexplored opportunity for primary prevention of degenerative brain diseases [71, 85, 91, 96].

Acknowledgments This work was supported in part by NIMH grants (MH51928; MH6357-01A1; and MH066029-01A2); an NIA Alzheimer's Disease Center Grant (AG 16570); funds received from the State of California, Department of Health Services, contract No. 013608-001; the Sidell-Kagan Foundation; and a Merit Review Grant from the Department of Veterans Affairs.

References

- Vonsattel JP, DiFiglia M (1998) Huntington disease. *J Neuro-pathol Exp Neurol* 57:369–384
- Li SH, Li XJ (2004) Huntingtin and its role in neuronal degeneration. *Neuroscientist* 10:467–475
- Landles C, Bates GP (2004) Huntingtin and the molecular pathogenesis of Huntington's disease. Fourth in molecular medicine review series. *EMBO Rep* 5:958–963
- Harper PS, Shaw D (1996) Huntington's disease: genetic and molecular studies. In: Harper PS (eds) *Huntington's disease* 2nd edn. W.B.Saunders, Philadelphia, pp 241–293
- Persichetti F, Carlee L, Faber PW, McNeil SM, Ambrose CM, Srinidhi J, Anderson M, Barnes GT, Gusella JF, MacDonald ME (1996) Differential expression of normal and mutant Huntington's disease gene alleles. *Neurobiol Dis* 3:183–190
- Bartzokis G, Cummings J, Perlman S, Hance DB, Mintz J (1999) Increased basal ganglia iron levels in Huntington disease. *Arch Neurol* 56:569–574
- Bartzokis G, Lu PH, Tishler TA, Perlman S (2006) In vivo assessment of iron in Huntington's disease and other age-related degenerative brain diseases. In: Sigel A, Sigel H, Sigel RKO (eds) *Metal ions in life sciences*, vol 1. Wiley, Chichester, pp 151–177
- Jones AL (1996) The Huntington's disease gene and its protein product. In: Harper PS (eds) *Huntington's disease*, 2 edn. W.B.Saunders, Philadelphia, pp 293–316
- Mascalchi M, Lolli F, Della Nave R, Tessa C, Petralli R, Gavazzi C, Politi LS, Macucci M, Filippi M, Piacentini S (2004) Huntington disease: volumetric, diffusion-weighted, and magnetization transfer MR imaging of brain. *Radiology* 232:867–873
- Jernigan TL, Salmon DP, Butters N, Hesselink JR (1991) Cerebral structure on MRI, Part II: specific changes in Alzheimer's and Huntington's diseases. *Biol Psychiatry* 29:68–81
- Aylward EH, Anderson NB, Bylsma FW, Wagster MV, Barta PE, Sherr M, Feeney J, Davis A, Rosenblatt A, Pearson GD, Ross CA (1998) Frontal lobe volume in patients with Huntington's disease. *Neurology* 50:252–258
- Mann DM, Oliver R, Snowden JS (1993) The topographic distribution of brain atrophy in Huntington's disease and progressive supranuclear palsy. *Acta Neuropathol (Berl)* 85:553–559
- Rosas HD, Koroshetz WJ, Chen YI, Skeuse C, Vangel M, Cudkovic ME, Caplan K, Marek K, Seidman LJ, Makris N, Jenkins BG, Goldstein JM (2003) Evidence for more widespread cerebral pathology in early HD: An MRI-based morphometric analysis. *Neurology* 60:1615–1620
- Thieben MJ, Duggins AJ, Good CD, Gomes L, Mahant N, Richards F, McCusker E, Frackowiak RS (2002) The distribution of structural neuropathology in pre-clinical Huntington's disease. *Brain* 125:1815–1828
- Fennema-Notestine C, Archibald SL, Jacobson MW, Corey-Bloom J, Paulsen JS, Peavy GM, Gamst AC, Hamilton JM, Salmon DP, Jernigan TL (2004) In vivo evidence of cerebellar atrophy and cerebral white matter loss in Huntington disease. *Neurology* 63:989–995
- Paulsen JS, Magnotta VA, Mikos AE, Paulson HL, Penziner E, Andreasen NC, Nopoulos PC (2006) Brain structure in preclinical Huntington's disease. *Biol Psychiatry* 59:57–63
- Reading SA, Yassa MA, Bakker A, Dziorny AC, Gourley LM, Yallapragada V, Rosenblatt A, Margolis RL, Aylward EH, Brandt J, Mori S, van Zijl P, Bassett SS, Ross CA (2005) Regional white matter change in pre-symptomatic Huntington's disease: a diffusion tensor imaging study. *Psychiatry Res* 140: 55–62
- Bruyn GW (1973) Neuropathological changes in Huntington's chorea. In: Barbeau A, Chase TN, Paulson GW (eds) *Huntington's Chorea*, vol 1. Raven Press, New York, pp 399–403
- Liss L, Paulson GW, Sommer A (1973) Rigid form of Huntington's chorea: a clinicopathological study of three cases. In: Barbeau A, Chase TN, Paulson GW (eds) *Huntington's Chorea*, vol 1. Raven Press, New York, pp 405–424
- Klintworth GK (1973) Huntington's chorea—morphologic contributions of a century. In: Barbeau A, Paulson GW, Chase TN (eds) *Advances in neurology. Huntington's chorea*, vol 1. 1872–1972. Raven Press, New York, pp 353–368
- de la Monte SM, Vonsattel JP, Richardson EP Jr (1988) Morphometric demonstration of atrophic changes in the cerebral cortex, white matter, and neostriatum in Huntington's disease. *J Neuropathol Exp Neurol* 47:516–525
- Peters A, Sethares C (2004) Oligodendrocytes, their progenitors and other neuroglial cells in the aging primate cerebral cortex. *Cereb Cortex* 14:995–1007
- Sotrel A, Paskevich PA, Kiely DK, Bird ED, Williams RS, Myers RH (1991) Morphometric analysis of the prefrontal cortex in Huntington's disease. *Neurology* 41:1117–1123
- Myers RH, Vonsattel JP, Paskevich PA, Kiely DK, Stevens TJ, Cupples LA, Richardson EP Jr, Bird ED (1991) Decreased neuronal and increased oligodendroglial densities in Huntington's disease caudate nucleus. *J Neuropathol Exp Neurol* 50:729–742
- Gomez-Tortosa E, MacDonald ME, Friend JC, Taylor SA, Weiler LJ, Cupples LA, Srinidhi J, Gusella JF, Bird ED, Vonsattel JP, Myers RH (2001) Quantitative neuropathological changes in presymptomatic Huntington's disease. *Ann Neurol* 49:29–34
- Bartzokis G (2004) Age-related myelin breakdown: a developmental model of cognitive decline and Alzheimer's disease. *Neurobiol Aging* 25:5–18
- Zecca L, Youdim MB, Riederer P, Connor JR, Crichton RR (2004) Iron, brain ageing and neurodegenerative disorders. *Nat Rev Neurosci* 5:863–873
- Dexter DT, Jenner P, Schapira AH, Marsden CD (1992) Alterations in levels of iron, ferritin, and other trace metals in neurodegenerative diseases affecting the basal ganglia. The Royal Kings and Queens Parkinson's Disease Research Group. *Ann Neurol* 32(Suppl 1): S94–S100
- Chen JC, Hardy PA, Kucharczyk W, Clauberg M, Joshi JG, Vourlas A, Dhar M, Henkelman RM (1993) MR of human postmortem brain tissue: correlative study between T2 and assays of iron and ferritin in Parkinson and Huntington disease. *AJNR Am J Neuroradiol* 14:275–281
- Youdim MB, Ben-Shachar D, Riederer P (1991) Iron in brain function and dysfunction with emphasis on Parkinson's disease. *Eur Neurol* 31(Suppl 1):34–40

31. Connor JR, Benkovic SA (1992) Iron regulation in the brain: histochemical, biochemical, and molecular considerations. *Ann Neurol* 32(Suppl 1):S51–S61
32. Connor JR, Menzies SL (1995) Cellular management of iron in the brain. *J Neurol Sci* 134(Suppl):33–44
33. Bartzokis G, Tishler TA, Shin I-S, Lu PH, Cummings JL (2004) Brain ferritin iron as a risk factor for age at onset in neurodegenerative diseases. In: LeVine S, Connor J, Schipper H (eds) *Redox-active metals in neurological disorders*, vol 1012. *Ann N Y Acad Sci*, New York, pp 224–236
34. Berg D, Youdim MB (2006) Role of iron in neurodegenerative disorders. *Top Magn Reson Imaging* 17:5–17
35. Oldendorf WH, Oldendorf W Jr (1988) *Basics of magnetic resonance imaging*. Martinus Nijhof Publishing, Boston, MA
36. Kamman RL, Go KG, Brouwer W, Berendsen HJ (1988) Nuclear magnetic resonance relaxation in experimental brain edema: effects of water concentration, protein concentration, and temperature. *Magn Reson Med* 6:265–274
37. Bartzokis G, Aravagiri M, Oldendorf WH, Mintz J, Marder SR (1993) Field dependent transverse relaxation rate increase may be a specific measure of tissue iron stores. *Magn Reson Med* 29:459–464
38. Bartzokis G, Mintz J, Sultzer D, Marx P, Herzberg JS, Phelan CK, Marder SR (1994) In vivo MR evaluation of age-related increases in brain iron. *AJNR Am J Neuroradiol* 15:1129–1138
39. Vymazal J, Hajek M, Patronas N, Giedd JN, Bulte JW, Baumgarner C, Tran V, Brooks RA (1995) The quantitative relation between T1-weighted and T2-weighted MRI of normal gray matter and iron concentration. *J Magn Reson Imaging* 5:554–560
40. Vymazal J, Brooks RA, Patronas N, Hajek M, Bulte JW, Di Chiro G (1995) Magnetic resonance imaging of brain iron in health and disease. *J Neurol Sci* 134(Suppl 1):19–26
41. Peters A, Rosene DL, Moss MB, Kemper TL, Abraham CR, Tigges J, Albert MS (1996) Neurobiological bases of age-related cognitive decline in the rhesus monkey. *J Neuropathol Exp Neurol* 55:861–874
42. Bartzokis G, Sultzer D, Lu PH, Nuechterlein KH, Mintz J, Cummings J (2004) Heterogeneous age-related breakdown of white matter structural integrity: implications for cortical “disconnection” in aging and Alzheimer’s disease. *Neurobiol Aging* 25:843–851
43. Bartzokis G, Lu PH, Geschwind DH, Edwards N, Mintz J, Cummings JL (2006) Apolipoprotein E genotype and age-related myelin breakdown in healthy individuals: implications for cognitive decline and dementia. *Arch Gen Psychiatry* 63:63–72
44. Bartzokis G, Beckson M, Hance DB, Marx P, Foster JA, Marder SR (1997) MR evaluation of age-related increase of brain iron in young adult and older normal males. *Magn Reson Imaging* 15:29–35
45. Bartzokis G, Sultzer D, Mintz J, Holt LE, Marx P, Phelan CK, Marder SR (1994) In vivo evaluation of brain iron in Alzheimer’s disease and normal subjects using MRI. *Biol Psychiatry* 35:480–487
46. Vymazal J, Brooks RA, Baumgarner C, Tran V, Katz D, Bulte JW, Bauminger R, Di Chiro G (1996) The relation between brain iron and NMR relaxation times: an in vitro study. *Magn Reson Med* 35:56–61
47. Vymazal J, Zak O, Bulte JW, Aisen P, Brooks RA (1996) T1 and T2 of ferritin solutions: effect of loading factor. *Magn Reson Med* 36:61–65
48. Floyd RA, Carney JM (1993) The role of metal ions in oxidative processes and aging. *Toxicol Ind Health* 9:197–214
49. Morris CM, Candy JM, Oakley AE, Bloxham CA, Edwardson JA (1992) Histochemical distribution of non-haem iron in the human brain. *Acta Anat (Basel)* 144:235–257
50. Bartzokis G, Sultzer D, Cummings BJ, Holt LE, Hance DB, Henderson VW, Mintz J (2000) In vivo evaluation of brain iron in Alzheimer’s disease and normal controls using magnetic resonance imaging. *Arch Gen Psychiatry* 57:47–53
51. Bartzokis G, Tishler TA, Lu PH, Villablanca P, Altschuler LL, Carter M, Huang D, Edwards N, Mintz J (2007) Brain ferritin iron may influence age- and gender-related risks of neurodegeneration. *Neurobiol Aging* 28:414–423
52. Bulte JW, Miller GF, Vymazal J, Brooks RA, Frank JA (1997) Hepatic hemosiderosis in non-human primates: quantification of liver iron using different field strengths. *Magn Reson Med* 37:530–536
53. Bartzokis G, Cummings JL, Markham CH, Marmarelis PZ, Treciokas LJ, Tishler TA, Marder SR, Mintz J (1999) MRI evaluation of brain iron in earlier- and later-onset Parkinson’s disease and normal subjects. *Magn Reson Imaging* 17:213–222
54. Doraiswamy PM, Finefrock AE (2004) Metals in our minds: therapeutic implications for neurodegenerative disorders. *Lancet Neurol* 3:431–434
55. Ke Y, Ming Qian Z (2003) Iron misregulation in the brain: a primary cause of neurodegenerative disorders. *Lancet Neurol* 2:246–253
56. Lamantia AS, Rakic P (1990) Cytological and quantitative characteristics of four cerebral commissures in the rhesus monkey. *J Comp Neurol* 291:520–537
57. Kemper T (1994) Neuroanatomical and neuropathological changes during aging and dementia. In: Albert M, Knoefel J (eds) *Clinical neurology of aging* 2nd edn. Oxford University Press, New York, pp 3–67
58. Yakovlev PI, Lecours AR (1967) *Regional development of the brain in early life*. Blackwell Scientific Publications, Boston, pp 3–70
59. Hallgren B, Sourander P (1958) The effect of age on the non-haem iron in the human brain. *J Neurochem* 3:41–51
60. Hotelling H (1940) The selection of variates for use in prediction with some comments on the general problem of nuisance parameters. *Ann Math Stat* 11:271–283
61. Steiger JH (1980) Tests for comparing elements of a correlation matrix. *Psychol Bull* 87:245–251
62. Hartman BK, Agrawal HC, Agrawal D, Kalmbach S (1982) Development and maturation of central nervous system myelin: comparison of immunohistochemical localization of proteolipid protein and basic protein in myelin and oligodendrocytes. *Proc Natl Acad Sci USA* 79:4217–4220
63. Trotter JL, Wegescheide CL, Garvey WF (1984) Regional studies of myelin proteins in human brain and spinal cord. *Neurochem Res* 9:133–146
64. Schwob VS, Clark HB, Agrawal D, Agrawal HC (1985) Electron microscopic immunocytochemical localization of myelin proteolipid protein and myelin basic protein to oligodendrocytes in rat brain during myelination. *J Neurochem* 45:559–571
65. Tolwani RJ, Cosgaya JM, Varma S, Jacob R, Kuo LE, Shooter EM (2004) BDNF overexpression produces a long-term increase in myelin formation in the peripheral nervous system. *J Neurosci Res* 77:662–669
66. Du Y, Fischer TZ, Lee LN, Lercher LD, Dreyfus CF (2003) Regionally specific effects of BDNF on oligodendrocytes. *Dev Neurosci* 25:116–126
67. Djalali S, Holtje M, Grosse G, Rothe T, Stroth T, Grosse J, Deng DR, Hellweg R, Grantyn R, Hortnagl H, Ahnert-Hilger G (2005) Effects of brain-derived neurotrophic factor (BDNF) on glial cells and serotonergic neurones during development. *J Neurochem* 92:616–627
68. Gauthier LR, Charrin BC, Borrell-Pages M, Dompierre JP, Rangone H, Cordelieres FP, De Mey J, MacDonald ME, Lessmann V, Humbert S, Saudou F (2004) Huntingtin controls

- neurotrophic support and survival of neurons by enhancing BDNF vesicular transport along microtubules. *Cell* 118:127–138
69. Canals JM, Pineda JR, Torres-Peraza JF, Bosch M, Martin-Ibanez R, Munoz MT, Mengod G, Ernors P, Alberch J (2004) Brain-derived neurotrophic factor regulates the onset and severity of motor dysfunction associated with enkephalinergic neuronal degeneration in Huntington's disease. *J Neurosci* 24:7727–7739
 70. O'Kusky J, Colonnier M (1982) Postnatal changes in the number of astrocytes, oligodendrocytes, and microglia in the visual cortex (area 17) of the macaque monkey: a stereological analysis in normal and monocularly deprived animals. *J Comp Neurol* 210:307–315
 71. Bartzokis G (2004) Quadratic trajectories of brain myelin content: unifying construct for neuropsychiatric disorders. *Neurobiol Aging* 25:49–62
 72. LeVine SM, Macklin WB (1990) Iron-enriched oligodendrocytes: a reexamination of their spatial distribution. *J Neurosci Res* 26:508–512
 73. Quintana C, Bellefqih S, Laval JY, Guerquin-Kern JL, Wu TD, Avila J, Ferrer I, Arranz R, Patino C (2006) Study of the localization of iron, ferritin, and hemosiderin in Alzheimer's disease hippocampus by analytical microscopy at the subcellular level. *J Struct Biol* 153:42–54
 74. Dwork AJ (1995) Effects of diet and development upon the uptake and distribution of cerebral iron. *J Neurol Sci* 134(Suppl 1):45–51
 75. Connor JR, Menzies SL (1996) Relationship of iron to oligodendrocytes and myelination. *Glia* 17:83–93
 76. Erb GL, Osterbur DL, LeVine SM (1996) The distribution of iron in the brain: a phylogenetic analysis using iron histochemistry. *Brain Res Dev Brain Res* 93:120–128
 77. Hill JM, Switzer RC (1984) The regional distribution and cellular localization of iron in the rat brain. *Neuroscience* 11:595–603
 78. Sapp E, Kegel KB, Aronin N, Hashikawa T, Uchiyama Y, Tohyama K, Bhide PG, Vonsattel JP, DiFiglia M (2001) Early and progressive accumulation of reactive microglia in the Huntington disease brain. *J Neuropathol Exp Neurol* 60:161–172
 79. Pavese N, Gerhard A, Tai YF, Ho AK, Turkheimer F, Barker RA, Brooks DJ, Piccini P (2006) Microglial activation correlates with severity in Huntington disease: a clinical and PET study. *Neurology* 66:1638–1643
 80. Mehlhase J, Gieche J, Widmer R, Grune T (2006) Ferritin levels in microglia depend upon activation: modulation by reactive oxygen species. *Biochim Biophys Acta* 1763:854–859
 81. Zhang X, Surguladze N, Slagle-Webb B, Cozzi A, Connor JR (2006) Cellular iron status influences the functional relationship between microglia and oligodendrocytes. *Glia* 54:795–804
 82. O'Kusky J, Colonnier M (1982) A laminar analysis of the number of neurons, glia, and synapses in the visual cortex (area 17) of adult macaque monkeys. *J Comp Neurol* 210:278–290
 83. Bartzokis G, Beckson M, Lu PH, Nuechterlein KH, Edwards N, Mintz J (2001) Age-related changes in frontal and temporal lobe volumes in men: a magnetic resonance imaging study. *Arch Gen Psychiatry* 58:461–465
 84. Bartzokis G (2002) Schizophrenia: breakdown in the well-regulated lifelong process of brain development and maturation. *Neuropsychopharmacology* 27:672–683
 85. Bartzokis G (2005) Brain myelination in prevalent neuropsychiatric developmental disorders: primary and comorbid addiction. *Adolesc Psychiatry* 29:55–96
 86. Vonsattel JP, Myers RH, Stevens TJ, Ferrante RJ, Bird ED, Richardson EP Jr (1985) Neuropathological classification of Huntington's disease. *J Neuropathol Exp Neurol* 44:559–577
 87. Crapper McLachlan DR, Dalton AJ, Kruck TP, Bell MY, Smith WL, Kalow W, Andrews DF (1991) Intramuscular desferrioxamine in patients with Alzheimer's disease [published erratum appears in *Lancet* 1991 Jun 29;337(8757):1618] [see comments]. *Lancet* 337:1304–1308
 88. Ritchie CW, Bush AI, Mackinnon A, Macfarlane S, Mastwyk M, MacGregor L, Kiers L, Cherny R, Li QX, Tammer A, Carrington D, Mavros C, Volitakis I, Xilinas M, Ames D, Davis S, Beyreuther K, Tanzi RE, Masters CL (2003) Metal-protein attenuation with iodochlorhydroxyquin (clioquinol) targeting abeta amyloid deposition and toxicity in Alzheimer disease: a pilot phase 2 clinical trial. *Arch Neurol* 60:1685–1691
 89. Shin RW, Kruck TP, Murayama H, Kitamoto T (2003) A novel trivalent cation chelator feralex dissociates binding of aluminum and iron associated with hyperphosphorylated tau of Alzheimer's disease. *Brain Res* 961:139–146
 90. Kaur D, Yantiri F, Rajagopalan S, Kumar J, Mo JQ, Boonplueang R, Viswanath V, Jacobs R, Yang L, Beal MF, DiMonte D, Volitakis I, Ellerby L, Cherny RA, Bush AI, Andersen JK (2003) Genetic or pharmacological iron chelation prevents MPTP-induced neurotoxicity in vivo: a novel therapy for Parkinson's disease. *Neuron* 37:899–909
 91. Nguyen T, Hamby A, Massa SM (2005) Clioquinol down-regulates mutant huntingtin expression in vitro and mitigates pathology in a Huntington's disease mouse model. *Proc Natl Acad Sci USA* 102:11840–11845
 92. Newman MB, Arendash GW, Shytle RD, Bickford PC, Tighe T, Sanberg PR (2002) Nicotine's oxidative and antioxidant properties in CNS. *Life Sci* 71:2807–2820
 93. Finefrock AE, Bush AI, Doraiswamy PM (2003) Current status of metals as therapeutic targets in Alzheimer's disease. *J Am Geriatr Soc* 51:1143–1148
 94. Mi S, Miller RH, Lee X, Scott ML, Shulag-Morskaya S, Shao Z, Chang J, Thill GLevesque M, Zhang M, Hession C, Sah D, Trapp B, He Z, Jung V, McCoy JM, Pepinsky RB (2005) LINGO-1 negatively regulates myelination by oligodendrocytes. *Nat Neurosci* 8:745–751
 95. Youdim MB, Stephenson G, Ben Shachar D (2004) Ironing iron out in Parkinson's disease and other neurodegenerative diseases with iron chelators: a lesson from 6-hydroxydopamine and iron chelators, desferal and VK-28. *Ann NY Acad Sci* 1012:306–325
 96. Bartzokis G, Lu PH, Mintz J (2004) Quantifying age-related myelin breakdown with MRI: novel therapeutic targets for preventing cognitive decline and Alzheimer's disease. *J Alzheimers Dis* 6:S53–S59